



Cubic inclusions in 4H-SiC studied with ballistic electron-emission microscopy

Y. Ding, K.-B. Park, J. P. Pelz, K. C. Palle, M. K. Mikhov, B. J. Skromme, H. Meidia, and S. Mahajan

Citation: *Journal of Vacuum Science & Technology A* **22**, 1351 (2004); doi: 10.1116/1.1705644

View online: <http://dx.doi.org/10.1116/1.1705644>

View Table of Contents: <http://scitation.aip.org/content/avs/journal/jvsta/22/4?ver=pdfcov>

Published by the AVS: Science & Technology of Materials, Interfaces, and Processing

Articles you may be interested in

[Dependence of spontaneous polarization on stacking sequence in SiC revealed by local Schottky barrier height variations over a partially formed 8H-SiC layer on a 4H-SiC substrate](#)

Appl. Phys. Lett. **99**, 252102 (2011); 10.1063/1.3670329

[Valence band structure and band offset of 3 C - and 4 H - Si C studied by ballistic hole emission microscopy](#)

Appl. Phys. Lett. **89**, 042103 (2006); 10.1063/1.2218302

[Quantum well behavior of single stacking fault 3C inclusions in 4H-SiC p - i - n diodes studied by ballistic electron emission microscopy](#)

Appl. Phys. Lett. **87**, 232103 (2005); 10.1063/1.2138442

[Cubic polytype inclusions in 4H-SiC](#)

J. Appl. Phys. **93**, 1577 (2003); 10.1063/1.1534376

[Ballistic electron emission microscopy study of Schottky contacts on 6H- and 4H- SiC](#)

Appl. Phys. Lett. **72**, 839 (1998); 10.1063/1.120910



A PASSION FOR PERFECTION

PFEIFFER  VACUUM

 HiCube® Eco turbopump station

■ \$4,995 for complete dry vacuum pump station

Are you looking for a perfect vacuum solution?
Please contact us!

Cubic inclusions in 4H-SiC studied with ballistic electron-emission microscopy

Y. Ding, K.-B. Park, and J. P. Pelz^{a)}

Department of Physics, The Ohio State University, Columbus, Ohio 43210-1106

K. C. Palle, M. K. Mikhov, and B. J. Skromme

Department of Electrical Engineering and Center for Solid State Electronics Research, Arizona State University, Tempe, Arizona 85287-5706

H. Meidia and S. Mahajan

Department of Chemical and Materials Engineering and Center for Solid State Electronics Research, Arizona State University, Tempe, Arizona 85287-6006

(Received 8 October 2003; accepted 1 December 2003; published 20 July 2004)

High-temperature-processing-induced “double-stacking fault” cubic inclusions in 4H-SiC were studied with ballistic electron emission microscopy (BEEM). Large BEEM current and a ~ 0.53 eV local reduction in the Schottky barrier height (SBH) were observed where the inclusions intersect a Pt interface, confirming the quantum-well nature of the inclusions and providing nanometer scale information about local electronic behavior. Measured spatial variations in the BEEM current are related to the inclusion orientation and local surface step structure. An observation of an anomalously low SBH is discussed, suggesting the existence of a triple- or quadruple-stacking fault inclusion. © 2004 American Vacuum Society. [DOI: 10.1116/1.1705644]

I. INTRODUCTION

SiC is a very promising semiconductor material for high power, high frequency, and high-temperature device applications, thanks to its wide band gap, and excellent physical properties.¹ SiC can form in a great number of different structural polytypes that differ from each other in the stacking sequence of close-packed SiC bilayer basal planes, but with otherwise the same composition, same Si–C nearest neighbor bonding geometry, and almost the same lattice constant. The different polytypes have similar formation energy and (filled-state) valence-band energy and electronic structure, since the nearest-neighbor atomic bonding is essentially the same. However their (empty-state) conduction-band energy and electronic structure can be very different, resulting in band gaps ranging from ~ 2.36 eV for “cubic” 3C-SiC to ~ 3.23 eV for the common hexagonal 4H-SiC and ~ 3.33 eV for the rare 2H-SiC polytype. Recently, the long-term stability issue of SiC devices has received much attention after it was discovered that stacking fault (SF) formation² during room-temperature electrical stressing of 4H- and 6H-SiC *pn* diode structures^{3–5} or during high-temperature processing of 4H-SiC materials with heavily *n*-type epilayers⁶ or substrates^{7,8} caused significant changes to optical and electrical behavior. It was found that basal plane SFs in 4H-SiC host resulted in planar “cubic inclusions,” i.e., thin (< 1.5 nm) sheets with cubic 3C local stacking embedded in the 4H-SiC host (in the electrically stressed diodes, all the inclusions observed by TEM were found to be of the “single-SF” type^{5,9} while those observed in the high-temperature-processed material were all “double-SF” inclusions^{6,8,10}). It was proposed that these cubic inclusions should behave

as unique “structure-only” electron quantum wells (QWs),^{2,11–13} which are delimited *only* by a change in local stacking.

We have used ballistic electron emission microscopy (BEEM) to characterize individual double-SF cubic inclusions in thermally processed 4H-SiC⁷ epilayers. Our measurements directly confirm the QW nature of these inclusions by showing that they support propagating two-dimensional (2D) states with a 2D conduction band minimum (CBM) at an estimated energy of ~ 0.53 eV below the 4H-SiC bulk CBM.¹⁴ Here we focus on measured spatial variations of the local electronic properties of the inclusions, and speculate about how these variations could result from local variations of structure and/or geometry of the inclusions.

BEEM is a three-terminal extension of scanning tunneling microscopy (STM) that can probe the *local* electronic transport properties of M/S interfaces with nanometer-scale spatial resolution and < 10 meV energy resolution.¹⁵ Typically, a negative tip bias voltage $-V_T$ is applied relative to the metal to inject “hot” ballistic electrons into the metal, a fraction of which crosses the metal overlayer, surmounts the Schottky barrier (if they have sufficient energy), and is collected in the substrate as the BEEM current I_C . The local Schottky barrier height (SBH) and additional information of the semiconductor conduction band structure can be obtained by measuring a BEEM spectrum (i.e., a BEEM I_C-V_T curve) and fitting it to a well-established model.¹⁵

II. EXPERIMENT

The starting materials were 35-mm-diam 4H-SiC wafers purchased from Cree, Inc. that had a $2 \mu\text{m}$ lightly *n*-type N-doped ($1-1.5 \times 10^{17} \text{ cm}^{-3}$) epilayer on a heavily *n*-type N-doped ($\sim 3 \times 10^{19} \text{ cm}^{-3}$) Si-face substrate with an 8° surface miscut from the (1000) hexagonal close-packed basal

^{a)}Electronic mail: jpelz@mps.ohio-state.edu

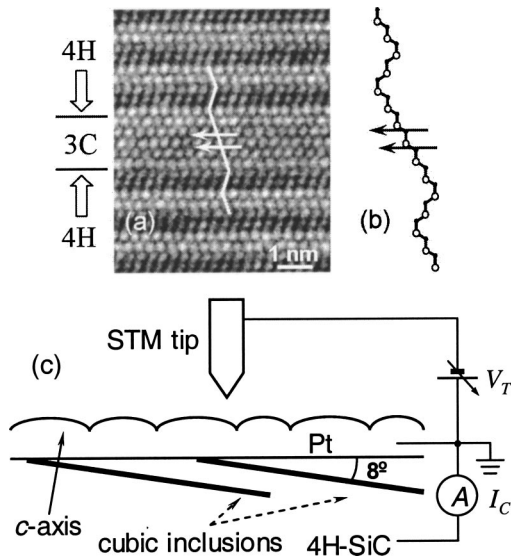


FIG. 1. (a) Cross-sectional TEM image of a cubic inclusion in 4H-SiC. Arrows indicate the two successive SFs that formed the inclusion. (b) Schematic illustration of the atomic stacking along the zigzagged line in (a). (c) Schematic illustration of BEEM experiment on our sample.

plane. After a 90 min dry oxidation at 1150 °C, many basal-plane cubic inclusions were found to have formed in the central part of the wafer, where the substrate happened to have a higher doping level.^{7,14} High-resolution cross-sectional TEM images [Figs. 1(a) and 1(b)] revealed that all the imaged cubic inclusions were of the double-stacking-fault type, and TEM and secondary electron imaging revealed that many of the inclusions extended all the way to the epilayer surface,^{7,10} as illustrated in Fig. 1(c). Macroscopic I - V and C - V measurements on metal-film diodes on the transformed region revealed a SBH reduction of ~ 0.41 – 0.47 eV, but with the same dependence on metal work function indicating a similar Schottky barrier pinning strength for the transformed and untransformed material.

Cleaved and oxide-stripped pieces from the transformed region of a wafer were then studied with BEEM. The wafer surface was cleaned and introduced into ultrahigh vacuum (UHV) as described in Ref. 14, and then two sets of 0.5-mm-diam Schottky diodes were made *in situ* by depositing ~ 8 and ~ 4 nm Pt films, respectively, through a shadow mask at room temperature using e-beam evaporation. Room temperature BEEM measurements [illustrated in Fig. 1(c)] were performed in an adjacent UHV chamber. A “tip locking” mechanism^{16,17} was implemented in our BEEM data acquisition program so that we may repeatedly measure BEEM spectra over the same locations on the samples (usually within a few nanometers). The UHV environment also enables us to make reproducible BEEM measurements on the same samples for many months.

III. RESULTS AND DISCUSSION

Most BEEM measurements on the transformed SiC samples measured at random locations show a local SBH of 1.54 ± 0.02 eV and a second CBM at ~ 0.13 eV above the

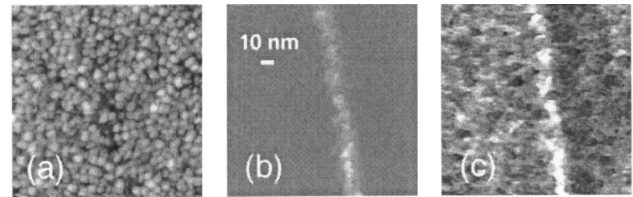


FIG. 2. (a) $(150 \text{ nm})^2$ STM image of an 8-nm-thick Pt film on transformed 4H-SiC, taken at $V_T = 1.5$ V and tunnel current of 5 nA. Gray scale: 4 nm. (b) Simultaneous BEEM image. The gray areas have zero BEEM current. (c) BEEM image over the same area taken at $V_T = 2.0$ V and tunnel current of 5 nA. The gray scale here is different than in (b), and BEEM current is everywhere from dark areas to bright areas.

first one. This is essentially the same behavior as found in earlier studies on normal Pt/4H-SiC contacts, which found a 1.58 ± 0.03 eV SBH and a second CBM at ~ 0.14 eV higher.¹⁸ However, if we search for BEEM current at a $V_T = 1.5$ V (just below the SBH of bulk 4H-SiC), we can easily locate where the 3C-SiC inclusions intersect the Pt-SiC interface. Figure 2(a) is a $(150 \text{ nm})^2$ STM topographic image of the top metal surface of a diode made with an 8-nm-thick Pt film, and shows no particularly distinctive features other than ~ 6 -nm-diam Pt crystallites, which are normal for polycrystalline thin metal films. Figure 2(b) is a simultaneously measured BEEM image (a plot of local BEEM current versus tip location) at $V_T = 1.5$ V, and shows a straight “stripe” of strongly enhanced BEEM current, but essentially no BEEM current elsewhere. The bright linear regions have reduced SBH as compared with bulk 4H-SiC, and correspond in spacing and orientation with cubic inclusions observed with TEM in the bulk and with secondary electron images of the transformed part of the bare wafer.^{7,14} BEEM spectra measured away from the high-BEEM stripes are always like those of normal Pt/4H-SiC contacts with a local SBH of 1.54 ± 0.02 eV (right-most curve in Fig. 3), confirming that $>95\%$ of the sample surface looks just like untransformed, bulk 4H-SiC. However, directly over the stripes, BEEM spectra yield a local SBH of 1.01 ± 0.03 eV (left-most curve in Fig. 3), which we found over all but one location on the >100 stripes on which BEEM spectra were measured (the sole exception will be discussed later).

Although not the major issue in this article, we believe that the measured ~ 0.53 eV local reduction in the SBH over an inclusion represents a reasonable estimate of the QW energy in an inclusion, i.e., the energy offset between the CBM of the 2D QW band and the host 4H-SiC bulk CBM. This is discussed in detail in Ref. 14, where we estimate a ~ 0.06 eV uncertainty in this energy, and address in detail the very important issue of how Schottky barrier pinning effects over the inclusions could affect quantitative estimates of the QW energy. Here we note that our estimate is in reasonable agreement with the 0.60 eV QW energy calculated by Iwata *et al.*¹³ for double-SF cubic inclusions in 4H-SiC. We also emphasize here that the measured local reduction in SBH is too large to be explained solely by a surface effect, such as a low barrier-height “patch” on an otherwise homogeneous substrate.¹⁹ But it is easily explained by a thin sheet of ma-

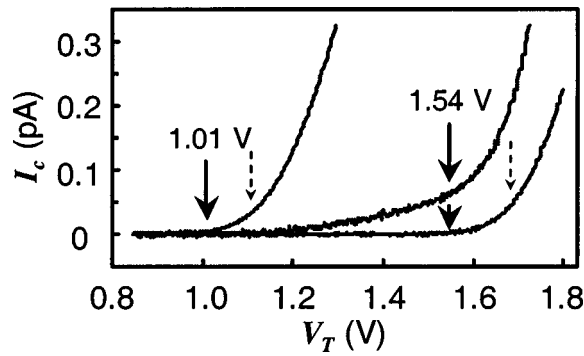


Fig. 3. Typical averaged BEEM I_C - V_T curves (average of 53 to 95 individual I_C - V_T curves at the same locations). Left: measured on an enhanced-BEEM stripe (scaled by a factor of 0.25). Right: away from a stripe. Middle: on the boundary of a stripe. Solid arrows indicate SBHs determined by fitting the data. Dashed arrows indicate the second thresholds. Fitted curves are not shown here because they are almost completely overlapped by the measured data.

terial with a lower energy conduction band (of propagating states) that intersects the metal interface, creating a lower-energy channel for BEEM electrons to conduct through the near-surface depletion region and into the substrate. This is illustrated in Fig. 4, which shows our calculated conduction-band potential energy profiles for a double-SF cubic inclusion intersecting a M/S interface, assuming the QW supports a 2D conduction band with its CBM at 0.53 eV below the 4H-SiC bulk CBM.

Around the stripe boundaries (middle curve in Fig. 3), BEEM spectra appear to be a superposition of a QW spectrum and a bulk 4H-SiC spectrum, with relative weights that depend on the distance of the tip from the inclusion. This is probably due to “spreading” of BEEM electrons in the metal film caused by multiple quasielastic scattering.²⁰ If we fit these boundary spectra as a superposition of two spectra, we obtain essentially the same two SBHs (~ 1.54 and ~ 1.01 eV) as found far from the inclusions and directly over them, respectively. Such a spreading of BEEM electrons is also consistent with measured BEEM profiles over the inclusions with $V_T = 1.5$ V, which show an apparent width of ~ 8 and ~ 10 nm for 4- and 8-nm-thick Pt film, respectively.¹⁴ This

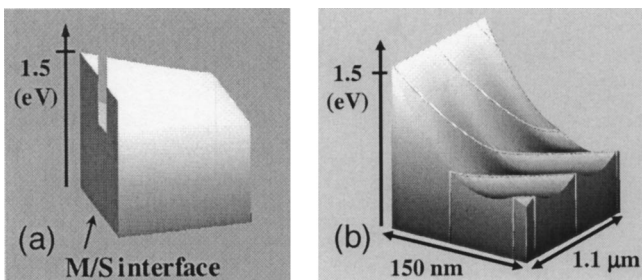


Fig. 4. Calculated potential profile near a Pt Schottky contact on 4H-SiC with double-SF inclusions, which shows QW 2D CBM extending into the bulk 4H-SiC along the inclusions. (a) Close-up view of a QW opening at the M/S interface. (b) Larger-scale view of the depletion region. Note that the QWs are partly filled deep in the bulk.

also suggests that the true width of the QW “opening” is significantly smaller than ~ 8 nm.

With regard to BEEM spectra measured over the inclusion, we have found that two BEEM thresholds in the Bell-Kaiser model¹⁵ are needed to get a good fit for many (but not all) of the BEEM spectra measured over inclusions. For example, the leftmost curve in Fig. 2(d) shows a BEEM spectrum measured over an inclusion, which can be fit extremely accurately by the Bell-Kaiser model if we assume two thresholds (the second threshold is indicated by the dashed arrow). The lowest threshold (which is the only threshold for some spectra) was always found to be $\sim 1.01 \pm 0.03$ eV (with the one exception discussed in the following). However, the second threshold varied greatly in energy (from 1.05 to ~ 1.3 eV), and the relative magnitude of BEEM current into this second transmission channel also varied greatly from one position to another. This is in contrast to the BEEM measurements over the 4H-SiC regions away from the inclusions, where a second threshold is always found at 1.67 ± 0.02 eV, with approximately the same relative weight (usually about three times as big as that of the first threshold). A second threshold is generally thought to be an indication of a higher energy CBM,¹⁵ and this second threshold for normal 4H-SiC corresponds to a known second CBM for 4H-SiC.¹⁸ We do not yet understand why a second threshold exists for some, but not all, areas over an inclusion.

We have found that the measured SBH over the 4H-SiC host is essentially the same (~ 1.54 eV) on either side of an inclusion, within our ~ 0.02 eV measurement uncertainty.¹⁴ However, we find that there is a clear asymmetry in the amplitude of the BEEM current into the 4H-SiC on one side of the inclusion compared to the other side. Figure 2(c) shows a BEEM image measured over the same area as in Figs. 2(a) and 2(b), but here with a tip bias $V_T = 2.0$ V, which is well above the SBH for the host 4H-SiC. The enhanced-BEEM stripe over the inclusion is still clearly identifiable, but the BEEM current over the host 4H-SiC is clearly smaller on the right side on an inclusion as compared to the left side, for a distance up to ~ 40 nm from the inclusion. We have observed a similar asymmetry in BEEM images around all inclusions whenever the tip bias is larger than the 4H-SiC SBH. Recall that the bright line in BEEM images is located where the planar inclusion intersects the metal interface. We suspect that this asymmetry in BEEM amplitude is due to the asymmetric geometry of the inclusion under the surface, which is inclined at a shallow $\sim 8^\circ$ angle down and to the right of the intersection line, as illustrated in Fig. 1(c). When the tip is to the left side of an inclusion, hot BEEM electrons injected into the 4H-SiC host do not encounter any subsurface inclusions close to the metal interface. In contrast, BEEM electrons injected to the right of the intersection line will encounter the planar inclusion immediately below the surface. It is likely that this QW inclusion enhances scattering of BEEM electrons back into the metal due to an unmatching impedance between bulk 4H-SiC and the inclusion, hence reducing the magnitude of the BEEM current to the immediate right side of all inclusion intersection lines.

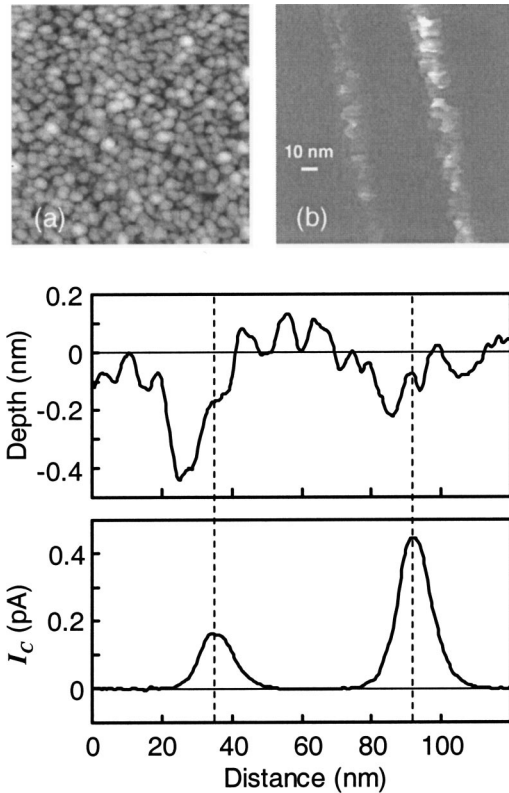


Fig. 5. (a) $(150 \text{ nm})^2$ STM image, taken at $V_T = 1.5 \text{ V}$ and tunnel current of 5 nA . Gray scale: 4 nm . (b) Simultaneous BEEM image. The gray areas have zero BEEM current. (c) Averaged STM topographic profile from (a). (d) Averaged BEEM current profile from (b). (c) and (d) are vertically aligned, and the dashed vertical lines indicate the location of the high-BEEM stripes.

We carefully measured the density of inclusions on two different Pt contacts, by sampling $\sim 5\%$ of the 0.5 mm contact diameter along a line perpendicular to the high-BEEM stripes. The average inclusion density was found to be $\sim 1.8/\mu\text{m}$ and $\sim 1.5/\mu\text{m}$ for the two contacts, although the total number of inclusions measured in this density survey was not big enough to be sure that this difference in measured inclusion density is statistically significant. The typical separation between inclusions was highly nonuniform, ranging from $>2 \mu\text{m}$ down to $\sim 60 \text{ nm}$ apart.

Figures 5(a) and 5(b) show a region where two inclusions happen to be only $\sim 60 \text{ nm}$ apart from each other (this corresponds to an $\sim 8 \text{ nm}$ separation along the c axis). Figures 5(c) and 5(d) are the averaged STM topographic and BEEM profiles over these the two inclusions, respectively. The topographic profile shows small topographic depressions ($<0.5 \text{ nm}$ deep), centered ~ 5 to 10 nm to the left of the center of the corresponding bright BEEM stripes. We find cubic inclusions are often associated with this kind of small topographic depressions, which are always found slightly to the left of the bright BEEM stripes. However, similar depressions were also observed at locations with no extra BEEM current or reduced barrier height. We suggest that these small topographic depressions are due to details of the local step structure of the vicinal SiC surface under the polycrystalline

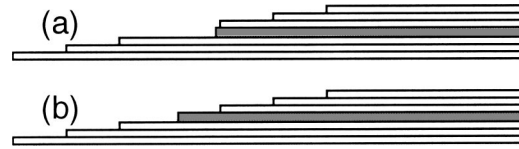


Fig. 6. Schematic illustration of the step structure on the vicinal SiC surface near the opening of a cubic inclusion (shaded bar), with two different configurations in (a) and (b).

Pt film, as shown schematically in Figs. 6(a) and 6(b) for two possible step arrangements. These figures assume $\sim 1.25 \text{ nm}$ width for the inclusion,²¹ and an $\sim 1 \text{ nm}$ atomic step height on the surrounding 4H-SiC vicinal basal plane surface,²² which is the stacking repeat length along the c axis.

Interestingly, the inclusion on the left-hand side of Fig. 5 has an obviously smaller BEEM current amplitude, but corresponds to a deeper topographic depression, as compared with the inclusion on the right-hand side. With reference to Fig. 6, it is easy to rationalize this behavior. If an inclusion happens to terminate close to the adjacent “uphill” 4H-SiC step [Fig. 6(a)], then one would expect a somewhat deeper-than-average topographic depression, as well as a smaller-than-average “opening” for electrons to enter the QW, resulting in a smaller BEEM amplitude. Note also that the topographic depression should be centered to the left of the QW opening, consistent with our observations. We also note that the measured SBH for the inclusion on the left-hand side is $1.01 \pm 0.02 \text{ eV}$, compared with $0.99 \pm 0.02 \text{ eV}$ over the other inclusion. This small but systematic difference in SBH is possibly related to the different geometry of the two inclusions’ openings at the M/S interface.

As discussed earlier, all inclusions we studied with BEEM had a measured SBH of $1.01 \pm 0.03 \text{ eV}$, with one notable exception. Around a particular location on one inclusion, we measured a SBH of $\sim 0.86 \text{ eV}$, or $\sim 0.15 \text{ eV}$ lower than all the rest. We note first that it is difficult to think of a tip artifact that could cause such a lowering in measured SBH, since tip-related artifacts should cause an *increase* in measure SBH (such as a tip with an insulating particle at its end) or a simple spatial smearing (such as a blunt or double tip). Energy conservation makes it difficult to imagine how a tip artifact could allow BEEM electrons to cross a Schottky barrier if the tip voltage is significantly less than the barrier height. Instead we suggest that this anomalously low SBH could be a real effect, resulting from a QW inclusion that is slightly wider than the predominant double-stacking fault inclusion. It is well established theoretically that wider cubic inclusions could exist (resulting from three, four, or more closely spaced stacking faults),²² and such wider cubic inclusions have been observed²³ (and sometimes intentionally produced)²⁴ in as-grown 4H-SiC. They are expected to be very rare in processed material because the formation energy is significantly larger than for single and double SF-induced inclusions.

However, if one did exist, it should have a significantly lower QW energy, due to reduced electron confinement. For example, Iwata *et al.*²¹ have calculated that the QW energy

of a triple-SF or quadruple-SF inclusion should be ~ 0.11 and ~ 0.15 eV lower than that of a double-SF inclusion, respectively. This is very similar to the ~ 0.15 eV lower SBH we measured over this particular location. Interestingly, BEEM measurements over other locations on the enhanced-BEEM stripe that contains this patch of particularly low SBH yielded the “normal” SBH of ~ 1.01 eV. This suggests that only a small segment of this inclusion contains one or more additional SFs other than the two faults found throughout the inclusion.

IV. SUMMARY

We have used BEEM to directly identify and characterize individual double-SF cubic inclusions in 4H-SiC, confirming that the inclusions support propagating states with a 2D CBM at an estimated ~ 0.53 eV below the bulk 4H CBM. Asymmetric spatial variations in the BEEM current across the inclusion openings are interpreted as the result of the inclusions’ tilted orientation relative to the M/S interface, and different BEEM current amplitude over different inclusions are found to be related to the local surface step structure. The observation of an anomalously low SBH is also discussed, suggesting the existence of three or four SFs along a small segment of an inclusion that contains two SFs elsewhere.

ACKNOWLEDGMENTS

The authors thank H. Iwata for helpful discussions. The work at The Ohio State University was supported by the Office of Naval Research under Grant No. N00014-93-1-0607 and the National Science Foundation under Grant No. DMR-0076362. The work at Arizona State University was supported by the National Science Foundation under Grant No. ECS-0080719, and by a Motorola Semiconductor Products Sector Sponsored Project.

¹E. Janzén, O. Kordina, A. Henry, W. M. Chen, N. T. Son, B. Monemar, E. Sörman, P. Bergman, C. I. Harris, R. Yakimova, M. Tuominen, A. O. Konstantinov, C. Hallin, and C. Hemmingsson, *Phys. Scr.*, T **54**, 283 (1994).

- ²M. S. Miao, S. Limpijumnong, and W. R. L. Lambrecht, *Appl. Phys. Lett.* **79**, 4360 (2001).
- ³H. Lendenmann, F. Dahlquist, N. Johansson, R. Söderholm, P. A. Nilsson, J. P. Bergman, and P. Skytt, *Mater. Sci. Forum* **353–356**, 727 (2001); J. P. Bergman, H. Lendenmann, P. A. Nilsson, U. Lindefelt, and P. Skytt, *ibid.* **353–356**, 299 (2001).
- ⁴A. Galeckas, J. Linnros, B. Breitholtz, and H. Bleichner, *Mater. Sci. Forum* **353–356**, 389 (2001); *J. Appl. Phys.* **90**, 980 (2001).
- ⁵J. Q. Liu, M. Skowronski, C. Hallin, R. Söderholm, and H. Lendenmann, *Appl. Phys. Lett.* **80**, 749 (2002).
- ⁶R. S. Okojie, M. Zhang, P. Pirouz, S. Tumakha, G. Jessen, and L. J. Brillson, *Appl. Phys. Lett.* **79**, 3056 (2001); L. J. Brillson, S. Tumakha, G. Jessen, R. S. Okojie, M. Zhang, and P. Pirouz, *ibid.* **81**, 2785 (2002).
- ⁷B. J. Skromme, K. Palle, C. D. Poweleit, L. R. Bryant, W. M. Vetter, M. Dudley, K. Moore, and T. Gehoski, *Mater. Sci. Forum* **389–393**, 455 (2002).
- ⁸J. Q. Liu, H. J. Chung, T. Kuhr, Q. Li, and M. Skowronski, *Appl. Phys. Lett.* **80**, 2111 (2002).
- ⁹P. O. A. Persson, L. Hultman, H. Jacobson, J. P. Bergman, E. Janzén, J. M. Molina-Aldareguia, W. J. Clegg, and T. Tuomi, *Appl. Phys. Lett.* **80**, 4852 (2002).
- ¹⁰B. J. Skromme, K. C. Palle, M. K. Mikhov, H. Meidia, S. Mahajan, X. R. Huang, W. M. Vetter, M. Dudley, K. Moore, S. Smith, and T. Gehoski, *Mater. Res. Soc. Symp. Proc.* **742**, 181 (2003).
- ¹¹S. G. Sridhara, F. H. C. Carlsson, J. P. Bergman, and E. Janzen, *Appl. Phys. Lett.* **79**, 3944 (2001).
- ¹²T. A. Kuhr, J. Q. Liu, H. J. Chung, M. Skowronski, and F. Szmulowicz, *J. Appl. Phys.* **92**, 5863 (2002).
- ¹³H. Iwata, U. Lindefelt, S. Oberg, and P. Briddon, *J. Phys.: Condens. Matter* **14**, 12733 (2002).
- ¹⁴Y. Ding, K.-B. Park, J. P. Pelz, K. C. Palle, M. K. Mikhov, B. J. Skromme, H. Meidia, and S. Mahajan, *Phys. Rev. B* **69**, 041305 (2004).
- ¹⁵W. J. Kaiser and L. D. Bell, *Phys. Rev. Lett.* **60**, 1406 (1988); L. D. Bell and W. J. Kaiser, *ibid.* **61**, 2368 (1988).
- ¹⁶B. S. Swartztruber, *Phys. Rev. Lett.* **76**, 459 (1996).
- ¹⁷B. Kaczer, Ph.D. thesis, The Ohio State University, Columbus, 1998.
- ¹⁸H.-J. Im, B. Kaczer, J. P. Pelz, S. Limpijumnong, W. R. L. Lambrecht, and W. J. Choyke, *J. Electron. Mater.* **27**, 345 (1998); B. Kaczer, H.-J. Im, J. P. Pelz, J. Chen, and W. J. Choyke, *Phys. Rev. B* **57**, 4027 (1998).
- ¹⁹R. T. Tung, *Phys. Rev. B* **45**, 13 509 (1992); *Appl. Phys. Lett.* **58**, 2821 (1991).
- ²⁰L. D. Bell, *Phys. Rev. Lett.* **77**, 3893 (1996).
- ²¹H. Iwata, U. Lindefelt, S. Oberg, and P. Briddon, *J. Appl. Phys.* **93**, 1577 (2003).
- ²²J. A. Powell, P. G. Neudeck, A. J. Trunek, G. M. Beheim, L. G. Matus, R. W. Hoffman, Jr., and L. J. Keys, *Appl. Phys. Lett.* **77**, 1449 (2000).
- ²³S. Bai, R. P. Devaty, W. J. Choyke, U. Kaiser, G. Wagner, and M. F. MacMillan, *Appl. Phys. Lett.* **83**, 3171 (2003).
- ²⁴A. Fissel, U. Kaiser, B. Schröter, W. Richter, and F. Bechstedt, *Appl. Surf. Sci.* **184**, 37 (2001).